Journal of Materials Chemistry C

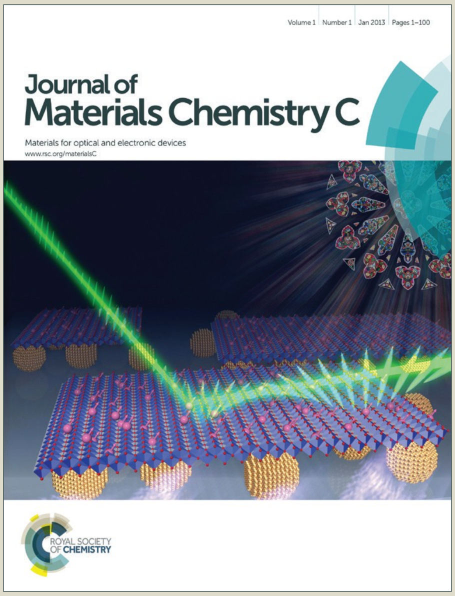

ROYAL SOCIETY OF CHEMISTRY

www.rsc.org/materialsC

Polymeric precursor for Solution-processed Amorphous Silicon Carbide

Takashi Masuda,*[1] Akira Iwasaka,[1] Hideyuki Takagishi,[2] and Tatsuya Shimoda[1]

[1] School of Material and Science, Japan Advanced Institute of Science and Technology, 1-1 Asahidai, Nomi, Ishikawa, 923-1292, Japan

[2] Faculty of Symbiotic System Science, Fukushima University, 1 Kanayagawa, Fukushima-shi, Fukushima, 960-1296, Japan

*Corresponding Author - mtakashi@jaist.ac.jp

Keywords: amorphous silicon carbide, solution process, polycarbosilane, polysilane

ABSTRACT

Amorphous silicon carbide (a-SiC) films are deposited via solution-based processes using a polymeric precursor solution consisting of polydihydrosilane with pendant hexyl groups. Unlike conventional polymeric precursors, this polymer neither requires catalysts nor oxidation for its synthesis and cross-linkage. Therefore, our polymeric precursor provides sufficient purity for the fabrication of solution-processed semiconducting a-SiC. Polymer-to-ceramic conversion is systematically investigated under various pyrolysis temperatures ranging from 320°C to 420°C. The polymer primarily undergoes cross-linking at temperatures above 150°C with increasing polymer fraction; this cross-linking is followed by carbon atoms being incorporated into an amorphous network at 380°C. The incorporated carbon atoms in the film are predominantly in the *sp*^{3}-bonding state with almost no amorphous graphite-like *sp*^{2} C=C clusters, leading to marked changes in the film's properties. The conductivity values of the resulting a-SiC films are comparable with those of semiconducting a-SiC films prepared using vacuum-based deposition.

1. Introduction

Amorphous silicon carbide (a-SiC) is an advanced material with high thermal conductivity, good chemical stability, and high mechanical strength. These attributes make a-SiC attractive for use as an alloy in advanced composites, mechanical abrasives, and electronic components.[1–5] Many researchers fabricate a-SiC by the thermal decomposition of polycarbosilane. This approach offers potential processing advantages over traditional solid-state methods because of the compatibility to solution processes, low decomposition temperature, and strong potential for the microstructural control of the ceramics.

Polycarbosilane is converted into a-SiC by heating.[6] The pyrolysis products of various other polysilanes, including poly(methylsilane), poly(silylenemethylene), and poly(silastyrene), have been investigated as starting materials for polycarbosilane.[7,8,9] Most of these previous studies have focused on structural and mechanical properties of polymers and the resultant SiC.[10] In contrast, the semiconductor properties of the resulting films are generally not considered because the prevention of oxidation,[11,12] contamination, and catalysis[13] during solidification and synthesis involving these precursors is difficult. Therefore, thermal decomposition of polycarbosilane has not been applied to the fabrication of a semiconducting SiC.

In this study, we synthesized a polymeric precursor for semiconducting SiC based on polydihydrosilane with pendant hexyl groups (PSH); the polymer is easily produced in one step from a mixture of cyclopentasilane (CPS: Si_5H_{10}) and 1-hexyne. An important feature of PSH is that the synthesis procedure and cross-linking neither require oxidation nor catalysts, resulting in highly pure SiC. Furthermore, a PSH transforms to a-SiC or polycrystalline SiC when heated under nitrogen gas at approximately 400°C or 1000°C, respectively.

These characteristics allow us to fabricate semiconducting a-SiC devices via solution processes. In general, semiconducting a-SiC films are deposited by expensive vacuum processes that use large amounts of hazardous gases, leading to low productivity and poor cost efficiency. Solution processes can overcome these problems because they require less-expensive vacuum-free equipment for handling liquid materials. These advantages of solution-processes and polymeric precursors for the generation of functional materials are widely-recognized for various fields.[14]

PSH offer substantial advantages over conventionally used polycarbosilanes. PSH enable the fabrication of solution-processed SiC electronics, as mentioned above. When PSH are used, the carbon content in the polymer skeleton can be controlled by changing the mixing ratio of CPS and carbon sources, leading to a high controllability of the Si/C stoichiometry in the resulting film. Moreover, PSH can be doped to form p- or n-type semiconductors by dissolving appropriate amounts of decaborane or white phosphorus, respectively, into liquid CPS before polymerization.[15] These features provide properties hitherto missing in SiC precursors.

The present research mainly aims to study the pyrolytic transformation from the polymeric precursor to a-SiC by increasing the pyrolysis temperatures T_p from 320°C to 420°C. The semiconductor properties of the resultant a-SiC films, including their optical, structural, and electrical properties, were investigated with the aid of polymer characterization. The clarification of the conversion of this polymer is the overriding key for enabling its use in electronics as a semiconducting material.

2. Experimental Section

Polymer preparation

CPS and its derived polymer were originally synthesized as a solution precursor for semiconducting silicon in our previous studies.[16,17] CPS was synthesized according to the method described in one of our previous studies[18] and was purified by vacuum distillation before use, as was 1-hexyne. Inductively coupled plasma mass spectrometry indicated that the concentrations of metal elements such as Li, Na, K, Rb, Cs, Fe, Be, Mg, Ca, Sr, Ba, Ti, Co, Cr, Cu, Mn, Mo, Ni, and Zn in CPS were less than 10 wt. ppb and that the Li concentration was 20–25 wt. ppb.

A PSH was synthesized by hydrosilylation and heat polymerization of a mixture of CPS and 1-hexyne at 50°C for 2 h, as shown in Scheme 1. The carbon content in the PSH was controlled by adjusting by the CPS-to-1-hexyne mole ratio to 75:25. All procedures were conducted in a nitrogen glove box with an oxygen content and a dew point less than 0.5 ppm and −75°C, respectively.

The relatively weak intrachain Si–Si bond in hydrosilane undergoes cleavage by heating, leading to a silylene-type radical.[19] Silylenes are important intermediates in the synthesis of hydrosilanes. They exist as ground-state singlets, and their characteristic reactions include insertion into Si–H and π-type addition across C=C and C≡C bonds.[20,21] Ab initio theoretical calculations of the reaction of SiH_2 with C_2H_4 indicate a reaction with no energy barrier, consistent with the high rate constants reported for these reactions.[22,23,24] In our case, the generated radical reacts with CPS by insertion into the Si–H bonds of CPS to form a larger polydihydrosilane. In addition, the polydihydrosilane incorporates a hexyl group via hydrosilylation between silylene and the unsaturated bond in 1-hexyne. The resultant PSH is a transparent, low-viscosity, liquid-state polymer.

Polymer analysis

The structure of the PSH was analyzed by Fourier transform infrared spectroscopy (FTIR), size-exclusion chromatography (SEC), and ^{29}Si nuclear magnetic resonance (NMR). The pyrolytic transformation from polymer to a-SiC was investigated using thermogravimetry and differential thermal analysis (TG/DTA). Infrared spectra were obtained using a Bruker Alpha spectrometer operated in the attenuated total reflectance mode for PSH and in the transmittance mode for coated films. The FTIR was installed in the glove box to minimize oxidation of the samples. Molecular weight (M_w) of the PSH was measured by SEC using an Agilent 1200 series chromatograph equipped with a Shodex KF-805 SEC column. The measurement conditions were the same as those reported in a previous study.[18] Cyclohexene was used as the mobile phase at a flow rate of 1 mL/min. The PSH solution was prepared at 3.0×10^{-3} g/mL in cyclohexene and filtered through a 0.45 μm Whatman filter prior to the injection of 150 μL samples. Solution-state ^{29}Si NMR spectra were obtained using Bruker Avance III (400 MHz) with toluene-d_8 as the solvent. The chemical shifts were referenced to tetramethylsilane (TMS). The samples were prepared in the glove box to prevent oxidation. The thermal analysis of the PSH was conducted using Seiko EXTRA TG/DTA 6200, which was also installed in the glove box to avoid exposing the samples to air. A heating rate of 20°C/min from 25°C to 450°C and a N_2 flow rate of 200 mL/min were used. Approximately 10 mg of the PSH was added dropwise onto an aluminum pan for the measurement.

a-SiC film analysis

The PSH dissolved in cyclooctane at a concentration of 20 vol.% was spin coated at 2000 rpm for 30 s onto quartz or silicon substrates. The PSH films were transformed into solid films at T_p ranging from 320°C to 420°C for 15 min using a hot plate under a nitrogen atmosphere to avoid the incorporation of oxygen into the films. The thickness of the resultant film was approximately 80 nm. The chemical bonding of the films were characterized by FTIR and X-ray photoelectron spectroscopy (XPS). The binding energy of Si 2p, C 1s, and O 1s was measured using Shimadzu Kratos AXIS ULTRA DLD. The film thickness and optical absorption coefficient were determined from transmittance and reflectance (TR) data collected using Scientific Computing International FilmTek 3000. The dark conductivity σ_d and photoconductivity σ_p at room temperature were measured using comb electrodes deposited onto the films. Al vapor deposition was employed for fabricating the comb electrodes whose gap length and width was 250 μm and 6 cm, respectively. Before Al deposition, the films were dipped in hydrofluoric acid (1%) to remove native oxide layers, followed by rinsed them in deionized water, and then they were dried by N_2 gas. The lateral current between the electrodes was measured using an Agilent 4155C semiconductor parameter analyzer under an applied voltage ranging from −10 to 10 V. An AM-1.5G solar simulator with an intensity of 100 mW/cm^2 was used for determining σ_p.

3. Results

Polymer analysis

The viscosity of the mixture of CPS and 1-hexyne gradually increased on heating at 50°C. The resultant viscous liquid was assumed to be a PSH, which was analyzed by SEC, FTIR, and NMR.

Figure 1 shows the RI chromatograms of the mixture of CPS and 1-hexyne with and without heat treatment at 50°C for 2 h. The chromatogram of the mixture without heat treatment exhibits a sharp peak at an elution volume of 12 mL. This position is consistent with that previously reported for CPS.[18] No peak corresponding to 1-hexyne was detected because of this compound's low M_w. In the case of the heated mixture, the chromatogram exhibits a broad peak at a lower elution volume and a weak peak at 12 mL, indicating that CPS was readily polymerized by heat treatment at 50°C. The relative M_w to polystyrene was 200–3000 g/mol.

The structure of the PSH was then investigated by FTIR. Figure 2(a) shows the FTIR spectra of the PSH. The spectra of CPS and 1-hexyne are also shown for comparison in Figures 2(b) and (c), respectively. The major peaks in the PSH spectra include bands at 570, 700, 850–900, 1450, and 2850–2950 cm^{-1}, which are attributed to the Si–Si wagging, Si–Si rocking, Si–H_2 bending, C–H bending, and C–$H_{2,3}$ stretching modes, respectively.[25] Because the PSH was synthesized by the heat polymerization of the mixture of CPS and 1-hexyne, the PSH spectra should be similar to the sum of the CPS and 1-hexyne spectra, with the exception of the appearance of the SiC-related peaks at 790 and 1600 cm^{-1} and the disappearance of the peaks at 3310 cm^{-1}. The peaks at 790, 1600, and 3310 cm^{-1} are assigned to the Si–C stretching, =C–H stretching, and ≡C–H stretching modes, respectively.[26,27] A clear peak at 3310 cm^{-1} in the 1-hexyne spectrum decreased in intensity in the PSH spectrum and new peaks related to Si–C and =C–H appeared in the PSH spectrum, indicating hydrosilylation between silicon and *sp* carbon.

The ^{29}Si NMR spectra of CPS and PSH are shown in Figure 3. The CPS spectrum shows a main peak at −106.9 ppm corresponding to Si–H_2. The small peak at −98.8 ppm is assigned to Si–H_3 in ring-opened CPS. In the PSH spectrum, new peaks appeared at −55.4 ppm and between −104 and −107.5 ppm in addition to the peaks of CPS. These new peaks are likely related to Si–C.

The chemical shifts were calculated at the B3LYP theory level using the 6-311++G** basis set and the Gaussian 09 program. Geometry optimizations were performed for a single molecule in vacuum. The calculated ^{29}Si NMR data of the PSH are summarized in Table 1, together with the experimental results. The molecular structure we determined is shown in the left of the table. The calculated and experimental data show good agreement, indicating that the peak at −55.4 ppm is attributable to a Si–C bond.

Thermal analysis of the PSH was used to illuminate pyrolysis. Figure 4 shows the TG, DTG, and DTA signals as functions of the heating temperature. The TG curve indicates a weight reduction of 54% when the PSH was heated to 420°C; consequently, 46% of the mass remained as a non-volatile material. The large weight loss near 300°C is associated with the desorption of the polymer fraction (Si_mH_n) that was generated by the cleavage of the framework of Si–Si bonds;[28] this framework was cleaved because of the lower bond energy of Si–Si bonds compared to the bond energies of other bonds such as Si–C, Si–H, C–H, and C–C.[29,30] Then, the framework of the C–C bonds was cleaved, leading to C_mH_n fractions as volatile materials. A decrease in carbon content in the films with higher T_p was confirmed by FTIR and XPS measurements, as mentioned later. Because of the evaporation of volatile materials such as CPS and small-molecule PSH, the DTA curve shows an endotherm at 25°C–150°C. In contrast, the exotherm at temperatures beyond 150°C indicates the partial transformation from a polymer to a cross-linked amorphous network along with the cleavage and recombination of Si–Si bonds: namely, liquid phase polymer transformed into solid phase intermediate. The elimination of hydrogen has been reported to occur prior to the evaporation of the Si_mH_n fractions in polydihydrosilane.[16] Therefore, it is interpreted that the starting point for the cross-linking in the films with lower T_p is dehydrogenated hydrosilane and a portion of the cleaved Si–Si sites. The significant cross-linking of the PSH occurs at approximately 380°C and is nearly complete above this temperature, as evident from the maximum exotherm peak at 380°C.

Film analysis

Optical properties

Figure 5(a) shows a photograph of the PSH films pyrolyzed at T_p = 320°C–420°C. Films with a thickness of 80 nm were coated onto glass substrates. The change in the color is attributed to a reduction of the optical gap E_g by network construction. The E_g was estimated from an equation $\alpha E = B(E - E_g)^2$, i.e., a Tauc plot, in which α is the optical absorption coefficient, B is a constant, and E is the photon energy in eV.[31] Figure 5(b) shows the Tauc plot, which indicates the E_g = 2.55, 2.36, 2.21, 2.15, and 2.11 eV for the films pyrolyzed at T_p = 340°C, 360°C, 380°C, 400°C, and 420°C, respectively. These E_g values for each T_p are 30% higher than those of solution-processed hydrogenated amorphous silicon (a-Si:H) films that are prepared using polydihyrosilane without pendant hexyl groups.[28]

It is reported that E_g of amorphous carbon lies in the 1.5–2.7 eV range, and the presence of sp^3 C–C bonds was insufficient to narrow the E_g, namely sp^2 sites contribute to produce the E_g in amorphous carbon.[32] Our films had few graphitic sp^2 sites, as discussed in the subsection of XPS and Raman measurement, indicating that the E_g of our films is determined by the Si–C bonds, not sp^3 C–C bonds. Therefore, it is interpreted for our films that the incorporation of carbon causes a shift of the band edge toward higher binding energies because the band gap is opened by the replacement of Si–Si bonds by stronger Si–C bonds. In contrast, the decrease of E_g with increasing T_p may be attributable to the network construction as well as the loss of the hydrogen atoms of the film, which is evident from the FTIR spectra, as mentioned in the next subsection. The decrease in hydrogen content causes a reduction in the chemical shift of the valence band to higher energy.[33]

FTIR measurements

The polymer-to-ceramic conversion was monitored by changes in the FTIR spectra of the PSH films pyrolyzed at T_p = 320°C–420°C, as shown in Figure 6. The spectrum of solution-processed a-Si:H film pyrolyzed at T_p = 420°C is also shown for comparison in the figure. The strong absorption peaks at 640, 2080–2100, and 2800–3000 cm^{-1} are attributed to the Si–H wagging, Si–$H_{1,2}$ stretching, and C–$H_{2,3}$ stretching modes, respectively.[17] Other weak absorption peaks at 760–790, 855–920, and

990 cm^{-1} are assigned to the Si–C stretching, $(Si–H_2)_n$ bending, and $C–H_n$ wagging modes, respectively.[34]

With increasing T_p, the Si–C peak at 790 cm^{-1} gradually decreased followed by the appearance of a broad peak with the center of 760 cm^{-1}. The peak at 760 cm^{-1} is assigned to a Si–C stretching mode in the a-SiC film,[35,36] whereas the peak at 790 cm^{-1} that appears in the spectrum of the film with lower T_p is assigned to a Si–C stretching mode in alkylsilanes.[26] The peak intensity at 760 cm^{-1} in our films with higher T_p is comparable with that in films prepared using vacuum-based equipment.[4] The strong peaks at 855–920 cm^{-1} with lower T_p means the existence of polymeric hydride $(SiH_2)_n$: PSH skeleton. The disappearance of the peaks for the films pyrolyzed at T_p ≥380°C indicates the transformation from a polymeric structure to a network structure by heating.

The decreasing peak intensities at 640, 2080–2100, and 2800–3000 cm^{-1} in the spectra of the films pyrolyzed at higher T_p indicates that the $Si–H_n$ and $C–H_n$ functionalities of the films were lost on heating. The direct cause of the decreasing peak intensities is dissociation of bonded H, as well as the desorption of fractions consisting of C_mH_n/Si_mH_n. However, the many hydrogen atoms are still remained as $Si– H_n$ and $C– H_n$ configurations even though the film is pyrolyzed at 420°C.

XPS and Raman measurements

The incorporation of carbon into the silicon films and the formation of Si–C bonds were analyzed by XPS. The films were etched by Ar^+ to remove surface contaminants before measurement. Figures 7 (a,b) show the Si 2p and C 1s bands of the PSH films pyrolyzed at 320 and 420°C. The spectrum of solution-processed a-Si:H film pyrolyzed at $T_p = 420$°C is also shown for comparison in the figure. The carbon and oxygen content was estimated using the integrated intensity of Si 2p, C 1s, and O 1s bands with relative sensitivity factors; the results indicate that the carbon content of the films at T_p = 320 and 420°C was 45 and 35 at.%, respectively, and the oxygen content for both films was < 2 at.%.

The Si 2p band in Figure 7(a) was decomposed into two components at binding energies of 99.5 and 100.3 eV because of the coexistence of Si–Si and Si–C bonds, respectively. [37] Figure 7 (c) shows the ratio of the Si–C bond to the total number of bonded Si in the film estimated from the integrated intensities of Si–Si (99.5 eV) and Si–C (100.3 eV) bands. The intensity of the Si–C peak at 100.3 eV increased substantially when $T_p \geq 380$°C, indicating that pyrolysis at $T_p \geq 380$°C resulted in the incorporation of carbon into the silicon network as Si–C bonds. Cross-linking involves the restructuring of the polymer backbone and the substantial cleavage of the hexyl groups to incorporate carbon atoms. The C 1s band in Figure 7(b) was decomposed into two components at binding energy of 282.4 and 283.5 eV for the film with T_p = 420°C, 283.5 and 284.8 eV for the film with T_p = 320°C. The binding energy at 282.4, 283.5, and 284.8 eV is attributed to carbon atoms as sp^3 C–Si, sp^2 C=Si, and sp^3 C–C, respectively.[37] The film with T_p = 320°C included many C–C bonds originated from the pendant hexyl groups in PSH. However, almost all carbon incorporated in the film with T_p = 420°C was bonded to Si as sp^3 C–Si, despite the presence of many C–C bonds in PSH. This disappearance of C–C bonds in the film with higher T_p is very interesting.

The a-SiC film prepared at T_p = 420°C was subsequently analyzed by Raman spectroscopy, as shown in Figure 8. The typical phonon bands of a-Si:H were observed at 150 and 480 cm^{-1}, which are attributed to first-order scattering by transverse acoustic and transverse optical bands, respectively. The energy tail in the 650–1700 cm^{-1} range is due to modes of tetrahedrally connected Si–C bonds.[38] The Raman spectrum of the pure carbon film includes a band centered at 1540 cm^{-1}, which is assigned to highly disordered graphitic carbon.[39] The absence of this band in the spectra of our films indicates a homogeneous distribution of carbon atoms involving mainly sp^3 bonding with Si or C atoms in the amorphous network. The Raman spectrum of our a-$Si_{1-x}C_x$ (x = 0.35) film shown in

Figure 8 is similar to Raman spectra of a-$Si_{1-x}C_x$ (x = 0.25) films prepared by the glow discharge chemical vapor deposition method,[39] which consist of an a-SiC structure of randomly distributed atoms.

I–V measurements

Typical values of σ_d and σ_p at room temperature are plotted in Figure 9 as functions of T_p. σ_d was almost constant and on the order of 10^{-12} S/cm, whereas σ_p increased with increasing T_p and then became constant at approximately 10^{-9} S/cm at $T_p \geq 380$°C. The conductivity of our a-SiC films is comparable with that of a-SiC films prepared using vacuum-based equipment.[40,41]

4. Discussion

Polymer structure

The incorporation of Si–C bonds into a polymeric precursor has been reported to be a requirement for the formation of films with these bonds.[15] Therefore, the origin of Si–C bonds in a polymer should be considered. The Si–C bonds in the PSH originated from the reaction between CPS and the C≡C bond in 1-hexyne. As in the case of 1-hexyne, 1-hexene also induced hydrosilylation and polymerization in the mixture, leading to the formation of a film with Si–C bonds. In contrast, the use of hexane instead of 1-hexyne/1-hexene as the carbon source led to the formation of a film with few Si–C bonds (results not shown). These results suggest that unsaturated (sp/sp^2) carbon in 1-hexyne/1-hexene plays an essential role in the formation of Si–C bonds in the resulting film, whereas saturated (sp^3) carbon does not induce hydrosilylation. Since the ring-opening energy of CPS is small,[42] the incorporation of Si–C bonds into the CPS skeleton would induce the ring opening and polymerization of CPS simultaneously.

Assuming that CPS reacts with the C≡C bond in 1-hexyne at a 1:1 molar ratio, the Si–C bond density in the PSH should increase until the number of moles of 1-hyxyne equals that of CPS, i.e., 50:50. However, hydrosilylation between CPS and the C≡C bond of 1-hexyne generates a C=C bond, introducing the possibility of second hydrosilylation; specifically, first and second hydrosilylation are induced by *sp* and sp^2 carbon, respectively. If 1-hexyne reacts twice with CPS via hydrosilylation, the Si–C bond density in the PSH should increase until the number of moles of 1-hyxyne equals half that of CPS, i.e., 33:67. Since the mixing ratio of 1-hexyne and CPS used in this study was 25:75, almost all 1-hexyne reacted with CPS in the case of either one or two hydrosilylation reactions. Therefore, we assumed that almost all 1-hexyne was consumed by hydrosilylation to construct the structure of $[(Si_5H_9)_3–C_6H_{11}]_{1–6}$ (M_w = 200–3000 g/mol) in the PSH in this study.

Polymer-to-ceramic conversion

The bond energy of Si–Si bonds is considerably lower than those of Si–C, Si–H, C–H, and C–C bonds.[29,30] In the conversion of the PSH to a-SiC, the scission of the $–(Si–Si)_n–$ chain to produce silyl/silylene-type radicals is proposed as a major radical source at a low temperature where a cross-linking of the PSH occurs. Fritz et al. proposed the mechanism for polysilanes prior to the re-formation of a $–(Si–C)_n–$ chain.[43] The radical species would initiate the cross-linking reaction at temperatures >150°C, as evidenced in the positive DTA curve in Figure 4. Moreover, the DTG peak at 300°C and the DTA peak at 380°C indicates that the considerable scission of the $–(Si–Si)_n–$ chain near 300°C produce many small fractions, leading to a large weight loss due to the evaporation of the fraction prior to the considerable cross-linking reaction at 380°C. The scission of the $–(Si–Si)_n–$ chain and the cross-linking reaction occur stepwise, as in the case of polydihydrosilane without hexyl side chains.[28]

Here, we make a comparison of Si–C bonds between the FTIR spectra in Figure 6 and the XPS chemical shifts in Figure 7. Although the FTIR spectra in the films with lower T_p had a clear peak at 790 cm^{-1} that related to Si–C stretching mode in alkylsilanes, XPS measurement resulted in few Si–C bonds in the films with $T_p < 380°C$. In contrast, the integrated intensities of the FTIR spectra at 760 cm^{-1} were proportionate to those of the Si–C band at 100.3 eV in XPS measurement. Therefore, it is interpreted that the absorption intensity/bond configuration of the Si–C stretching mode in alkylsilanes is different from that of Si–C stretching mode in a-SiC film.

As for the carbon configuration, it changed dramatically between 320 and 420°C. Although the carbon content in the films reduced from 45 at.% for $T_p = 320°C$ to 35 at.% for $T_p = 420°C$, the concentration of Si–C bonds increases abruptly at $T_p = 380°C$. The C–C bonds in pendant hexyl groups in PSH would be cleaved by thermal decomposition by heating, followed by a part of carbon atoms was evaporated as C_mH_n gasses, leaving behind cleaved carbon atoms and C–Si bonds in the film. The cleaved carbon atoms are then incorporated into the Si network as C–Si bonds through cross-linking at 380°C. Consequently, the C–Si bonds increased, even though the total amount of carbon decreased.

A polymer-to-ceramic conversion based on our results is summarized in Figure 10. The cleavage of Si–Si and Si–H bonds progresses prior to that of C–C bonds. The generated radical species induce the cross-linking to form an amorphous network construction at >150°C, followed by the carbon is incorporated into the network as C–Si bonds at 380°C. The a-SiC structure is described as a disordered a-Si network, in which carbon atoms are in an sp^3 C–Si configuration, and many hydrogen atoms are incorporated in the form of Si–H_n/C–H_n entities. The result of Raman measurement supports the proposed structure, in which the carbon atoms are preferentially homogeneously distributed, forming sp^3 bonds with Si in the amorphous network.

The effect of the structural transformation from PSH into a-SiC film are appeared as electrical properties in Figure 9. The σ_p increases until T_p = 380°C because the network structure is constructed by heating, followed by the σ_p becomes stable at higher T_p due to the stabilization of the network structure. As shown in Figure 4, TG/DTA curves also support that the a-SiC network become stable at $T_p > 380$°C.

In contrast, the values of σ_d are insensitive to the T_p. It cannot be assumed that there is no correlation between σ_d and structural changing. Other effects may compensate for alterations in σ_d. For instance, the evaporation of carbon species during the pyrolysis shifts the balance of Si/C stoichiometry. In addition, the higher T_p serves as an annealing effect to reduce the number of dangling bonds. Our film should contain many dangling bonds because the network structure is constructed by dehydrogenation of the $–(SiH_2)–$ skeleton. Therefore, further analysis of structural fluctuations, inhomogeneity, and defect density should be conducted to clarify the electrical properties.

5. Conclusion

In this study, we have emphasized that the pyrolytic transformation from PSH to a-SiC was realized at $T_p \geq 380$°C. The Si 2p and C 1s bands in XPS measurement offered direct evidence for the formation of Si–C bonds in the film. Moreover, the incorporated carbon widened the E_g from 1.68 eV (a-Si:H) to 2.11 (a-SiC) for the film with pyrolized at 420°C because of the replacement of Si–Si/Si–H bonds by the stronger Si–C bonds.

We also clarified the optical, structural, and electrical changes that occur during the pyrolysis of a PSH. These changes include extensive Si–Si, C–C, C–H, and Si–H bond cleavages and eventual consolidation of an a-SiC network. The bond cleavage induced the cross-linking to form an amorphous network construction at >150°C. In particular, carbon atoms were incorporated into the Si network as C–Si bonds at 380°C. Therefore, the pyrolytic transformation from a PSH to a-SiC near 380°C plays a critical role in the formation of a-SiC structure.

FTIR, XPS, and Raman spectra revealed structural details of polymer-to-ceramic conversion and provided insights into the chemical bonding. The structure of resultant a-SiC is described as a disordered a-Si network, in which carbon atoms are in sp^3 C–Si configuration, and many hydrogen atoms are incorporated in the form of Si–H_n/C–H_n entities. Carbon is effectively incorporated into the a-SiC film, and the increase in the number of Si–C bonds at T_p = 380°C leads to pronounced changes in the film's properties.

The information related to the polymer structure, polymer-to-ceramic conversion, and resultant a-SiC film should assist in the design of new ceramic precursors to satisfy specific objectives. A PSH has tailorable physical properties such as solubility, viscosity, and wettability for coating, which make it an attractive material for use in solution-processed SiC electronics.

ACKNOWLEDGMENT

This work was partially funded by the Izumi Science and Technology Foundation, the Mitani Foundation for Research and Development, and Grants-in-Aid for Scientific Research, Japan.

REFERENCES

[1] R. A. Street, *in Semiconductors and Semimetals*, ed. by J. Pankove, Vol 21, Part B, Academic, New York, **1984**.

[2] M. M. Rahman, C. Y. W. Yang, G. L. Harris, in *Amorphous and crystalline silicon carbide II*, Springer-Verlag, Berlin Heidelberg, **1988**.

[3] O. K. Porada, V. I. Ivashchenko, L. A. Ivashchenko, G. V. Rusakov, S. N. Dub, A. I. Stegnij, *Surf. Coat. Tech.* **2004**, 180–181, 122.

[4] Y. Tawada, K. Tsuge, M. Kondo, H. Okamoto, Y. Hamakawa, *J. Appl. Phys.* **1982**, 53, 5273.

[5] D. A. Anderson and W. E. Spear, *Phil. Mag.* **1977**, 35, 1.

[6] S. Yajima, J. Hayashi, M. Omori, *Chem. Lett.* **1975**, 931.

[7] Z. F. Zhang, F. Babonneau, R. M. Laine, Y. Mu, J. F. Harrod, J. A. Rahn, *J. Am. Ceram. Soc.* **1991**, 74, 670.

[8] Q. Liu, H. J. Wu, R. Lewis, G. E. Maciel, L. V. Interrante, *Chem. Mater.* **1999**, 11, 2038.

[9] R. West, L. D. David, P. I. Djurovich, H. Yu, R. Sinclair, *Am. Ceram. Soc. Bull.* **1983**, 62, 899.

[10] Y. Hasegawa and K. Okamura, *J. Mater. Sci.* **1983**, 18, 3633.

[11] Y. Hasegawa, M. Iimura, S. Yajima, *J. Mater. Sci.* **1980**, 15, 720.

[12] C. Laffon, A. M. Flank, P. Lagarde, M. Laridjani, R. Hagege, P. Olry, J. Cotteret, J. Dixmier, J. L. Miquel, H. Hommel, A. P. Legrand, *J. Mater. Sci.* **1989**, 24, 1503.

[13] S. Yajima, Y. Hasegawa, K. Okamura, T. Matsuzawa, *Nature* **1978**, 273 525.

[14] Q. Dong, G. Li, C. -L. Ho, M. Faisal, C. -W. Leung, P. W. -T. Pong, K. Liu, B. -Z. Tang, I. Manners, W. -Y. Wong, *Adv. Mater.* **2012**, 24, 1034.; Q. Dong, G. Li, C. -L. Ho, C. -W. Leung, P. W.

-T. Pong, I. Manners, W. -Y. Wong, *Adv. Func. Mater.* **2014**, 24, 857.; Q. Dong, G. Li, H. Wang, P. W. -T. Pong, C. -W. Leung, I. Manners, C. -L. Ho, H. Li, W. -Y. Wong, *J. Mater. Chem. C* **2015**, 3, 734.; K. Liu, C. -L. Ho, S. Aouba, Y. -Q. Zhao, Z. -H. Lu, S. Petrov, N. Coombs, P. Dube, H. E. Ruda, W. -Y. Wong, I. Manners, *Angew. Chem. Int. Ed.* **2008**, 47, 1255.; G. Li, Q. Dong, J. Xin, C. W. Leung, P. T. Lai, W. -Y. Wong, P. W. T. Pong, *Microelectron. Eng.* **2013**, 110, 192,; C. -L. Ho, S. -Y. Poon, K. Liu, C. -K. Wong, G. -L. Lu, S. Petrov, I. Manners, W. -Y. Wong, *J. Organomet. Chem.* **2013**, 744, 165.

[15] T. Masuda, Z. Shen, H. Takagishi, K. Ohdaira, T. Shimoda, *Jpn. J. Appl. Phys.* **2014**, 53, 031304. (Only p-type a-SiC is mentioned)

[16] T. Shimoda, Y. Matsuki, M. Furusawa, T. Aoki, I. Yudasaka, H. Tanaka, H. Iwasawa, D. Wang, M. Miyasaka, Y. Takeuchi, *Nature* **2006**, 440, 83.

[17] T. Masuda, N. Sotani, H. Hamada, Y. Matsuki, T. Shimoda, *Appl. Phys. Lett.* **2012**, 100, 253908.

[18] T. Masuda, Y. Matsuki, T. Shimoda, *Polymer* **2012**, 53, 2973.

[19] T. R. Dietrich, S. Chiussi, M. Marek, A. Roth, F. J. Comes, *J. Phys. Chem.* **1991**, 95, 9302.

[20] P. P. Gaspar, in *Reactive Intermediates*, (Eds. M. Jones Jr. and R. A. Moss), Wiley, New York **1978**, 1, 229; **1981**, 2, 335; **1985**, 3, 333.

[21] Y. N. Tang, in *Reactive Intermediates* (Ed. R. A. Abramovitch), Plenum, New York **1982**, 2, 297.

[22] F. Anwari and M. S. Gordon, *Isr. J. Chem.* **1983**, 23, 129.

[23] G. Inoue and M. Suzuki, *Chem. Phys. Lett.* **1985**, 122, 361.

[24] J. O. Chu, D. B. Beach, J. M. Jasinski, *J. Phys. Chem.* **1987**, 91, 5340.

[25] M. H. Brodsky, M. Cardona, J. J. Cuomo, *Phys. Rev. B* **1977**, 16, 3556.

[26] H. Murata, H. Matsuura, K. Ohno, T. Sato, *J. Mol. Struct.* **1979**, 52, 1.

[27] S. Liu, S. Gangopadhyay, G. Sreenivas, S. S. Ang, H. A. Naseem, *Phys. Rev. B* **1997**, 55, 13020.

[28] T. Masuda, Y. Matsuki, T. Shimoda, *Thin Solid Films* **2012**, 520, 6603.

[29] M. L. Huggins, *J. Am. Chem. Soc.* **1953**, 75, 4123.

[30] S. Yajima, Y. Hasegawa, J. Hayashi, M. Iimura, *J. Mater. Sci.* **1978**, 13, 2569.

[31] J. Tauc and R. Grigorovici, A. Vancu, *Phys. Stat. Sol.* **1966**, 15, 627.

[32] J. Robertson and E. P. O'Reilly, *Phys. Rev, B* **1987**, 35, 2946.

[33] J. I. Pankove, in *Semiconductors and Semimetals, "Hydrogeated Amorphous Silicon" Part A*, Academic Press, Orlando and London, **1984**, 21.

[34] H. Wieder, M. Cardona, C. R. Guarnieri, *Phys. Status Solidi (b)* **1979**, 92, 99.

[35] Y. Katayama, K. Usami, T. Shimada, *Philos. Mag. B* **1981**, 43, 283.

[36] Y. Catherine and G. Turban, *Thin Solid Films* **1980**, 70, 101.

[37] Y. H. Wang, J. Lin, and C. H. A. Huan, *Mater. Sci. Eng. B* **2002**, 95, 43.

[38] A. Chehaidar, R. Carles, A. Zwick, C. Meunier, B. Cros, J. Durand, *J. Non-Cryst. Solids* **1994**, 169, 37.

[39] F. Tuinstra and J. L. Koenig, *J. Chem. Phys.* **1970**, 53, 1126.

[40] D. M. Bhusari and S. T. Kshirsagar, *J. Appl. Phys.* **1993**, 73, 1743.

[41] H. Matsumura, T. Uesugi, H. Ihara, *Jpn. J. Appl. Phys.* **1985**, 24, L24.

[42] A. Sugiyama, T. Shimoda, D. H. Chi, *Mol. Phys.* **2010**, 108, 1649.

[43] G. Fritz, J. Grobe, D. Kummer, *Adv. Inorg, Chem. Radiochem.* **1965**, 7, 349.

Figure caption

Figure 1. RI chromatograms of the mixture of CPS and 1-hexyne with and without heat treatment at 50°C for 2 h, as determined by SEC.

Figure 2. Fourier transform infrared spectra obtained in attenuated total reflectance mode: (a) PSH, (b) CPS, and (c) 1-hexyne.

Figure 3. Solution ^{29}Si NMR spectra: (a) CPS and (b) PSH.

Figure 4. TG (red line), DTA (blue line), and DTG (black line) curves of PSH as a function of heating temperature under a nitrogen atmosphere.

Figure 5.(a) Photographic image of PSH films coated onto 2×2 cm^2 glass substrates. The films were pyrolyzed at 320°C–420°C for 15 min. (b) Tauc plot of the PSH films with experimental data (opened circles) and the fitted line (solid line).

Figure 6. FTIR absorption spectra of PSH films prepared at various pyrolysis temperatures: (a) 320°C, (b) 340°C, (c) 360°C, (d) 380°C, (e) 400°C, (f) 420°C, and (g) 420°C (a-Si:H).

Figure 7 (a–b). Si 2p and C 1s peaks of PSH films pyrolyzed at 320°C and 420°C. The a-Si:H film pyrolyzed at 420°C is also shown as a reference. The closed circles and solid lines represent experimental and fitted data, respectively. (c) The ratio of Si–C bond to the total number of bonded Si in the film: [Si–C]/([Si–Si] + [Si–C]), estimated from Si–Si and Si–C bands at 99.5 and 100.3 eV, respectively, for the film with various pyrolysis temperatures.

Figure 8. Raman spectrum of PSH films pyrolyzed at 420°C.

Figure 9. Dark conductivity and photoconductivity of PSH films treated at various pyrolysis temperatures.

Figure 10. Conversion process of PSH into a-SiC.

Scheme 1. Synthesis route for polydihydrosilane with pendant hexyl groups (PSH) from a mixture of cyclopentasilane (CPS) and 1-hexyne.

Table 1. Calculated and experimental ^{29}Si NMR chemical shifts in toluene-d_8; chemical shifts are stated relative to TMS.

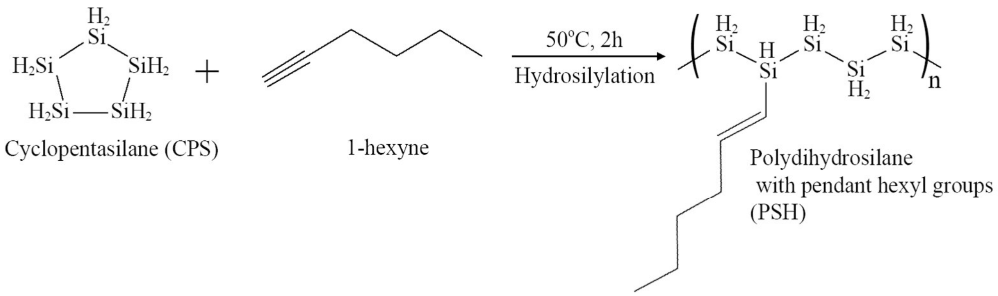

141x40mm (300 x 300 DPI)

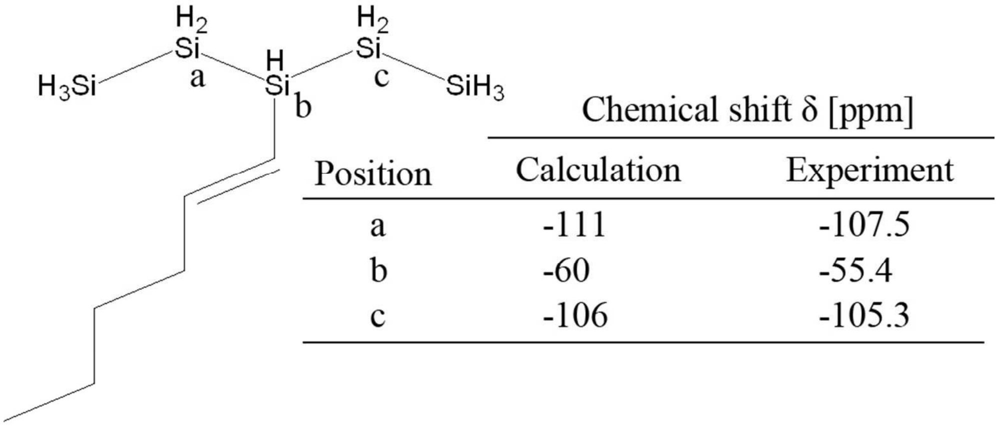

	Chemical shift δ [ppm]	
Position	Calculation	Experiment
a	-111	-107.5
b	-60	-55.4
c	-106	-105.3

88x39mm (300 x 300 DPI)

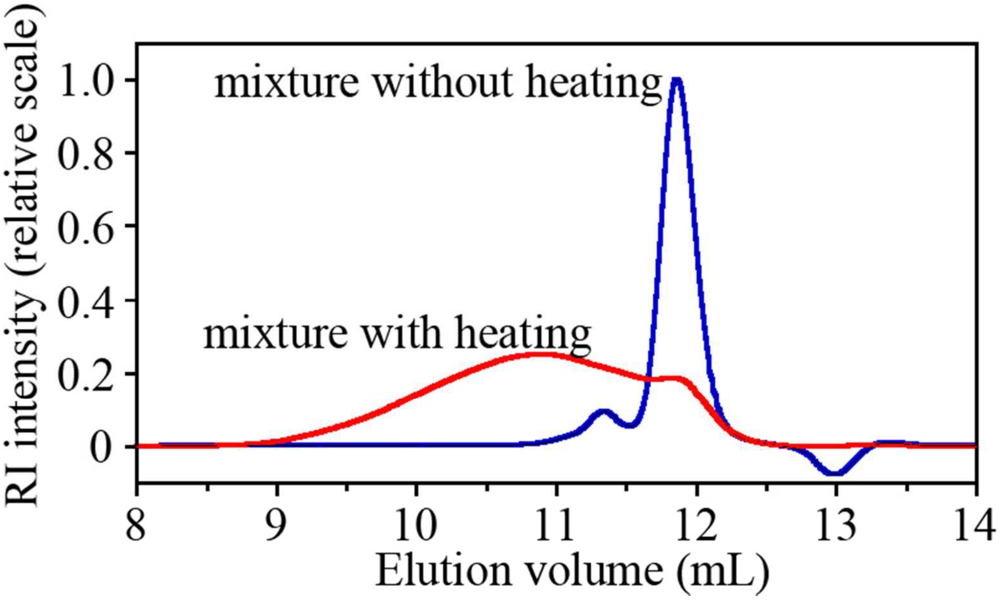

68x40mm (300 x 300 DPI)

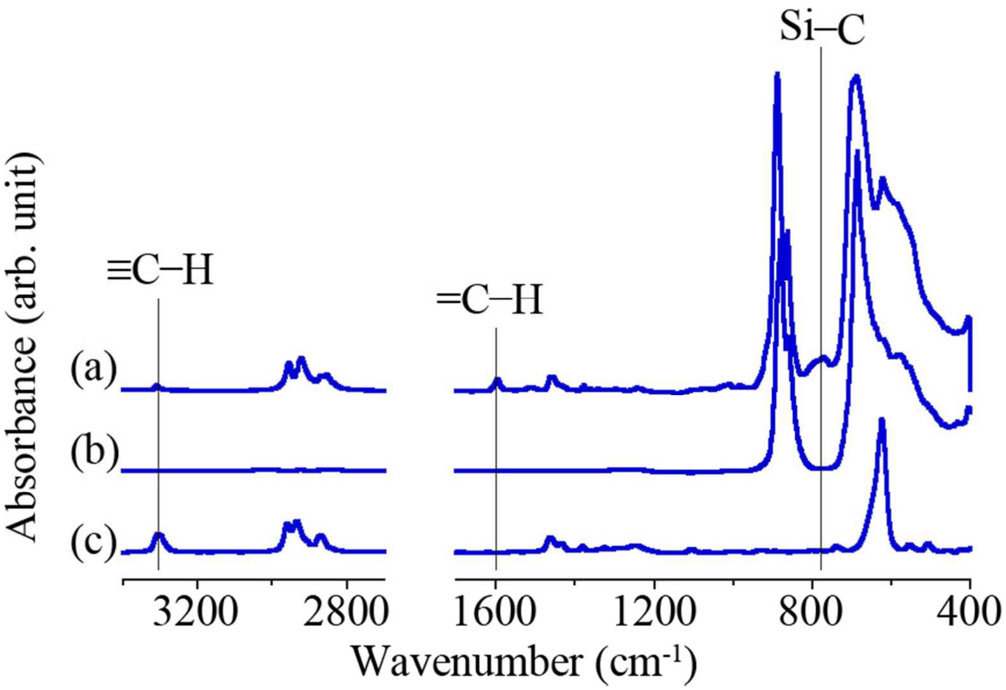

72x49mm (300 x 300 DPI)

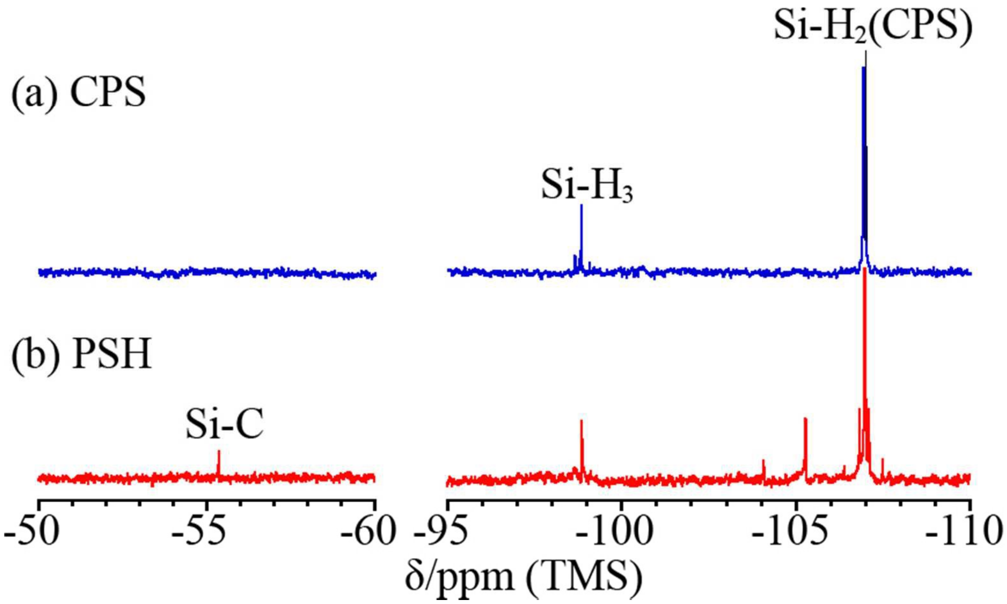

73x43mm (300 x 300 DPI)

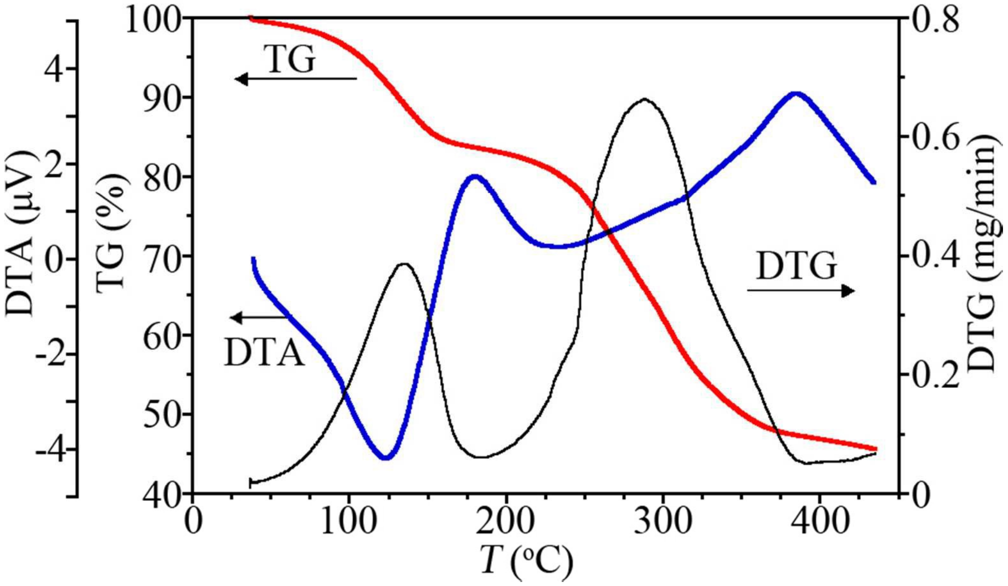

79x46mm (300 x 300 DPI)

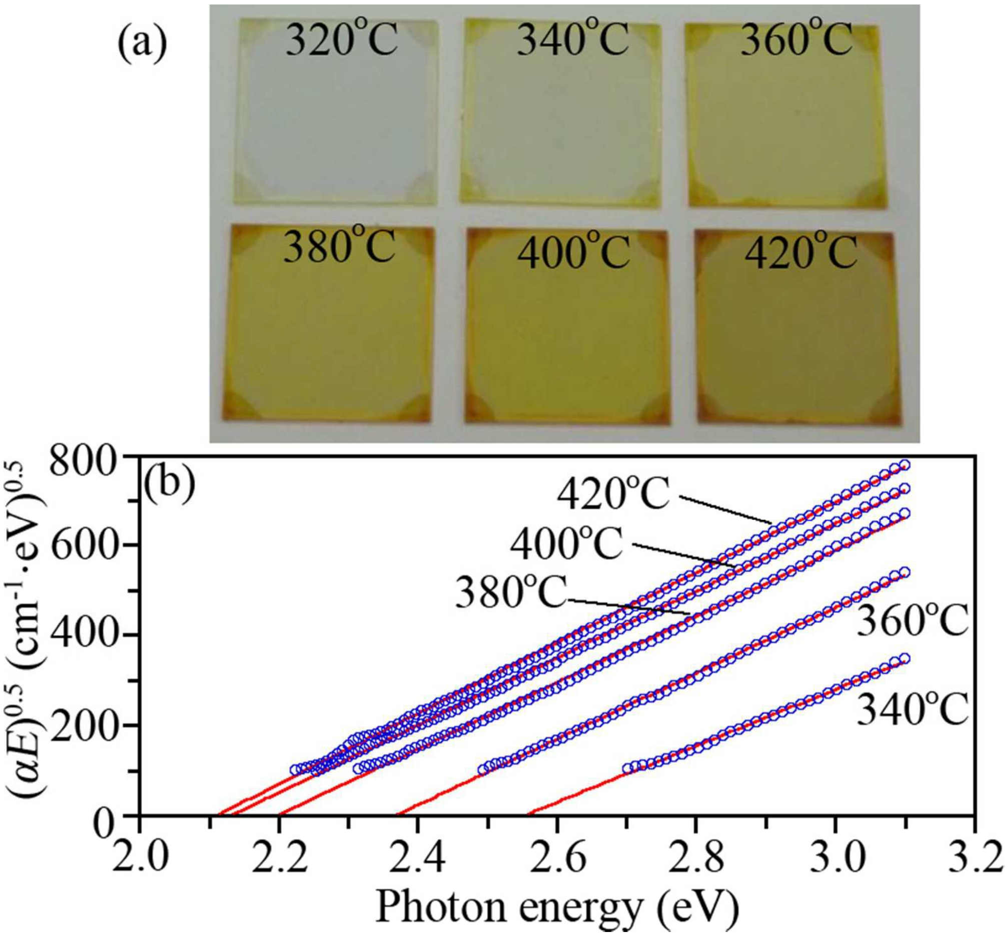

68x63mm (300 x 300 DPI)

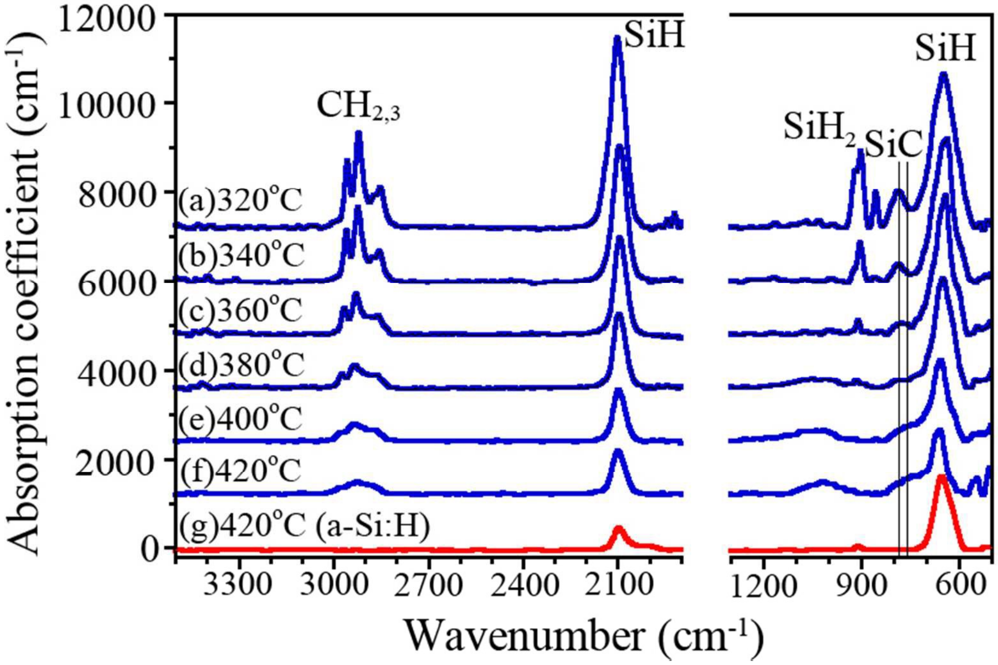

70x46mm (300 x 300 DPI)

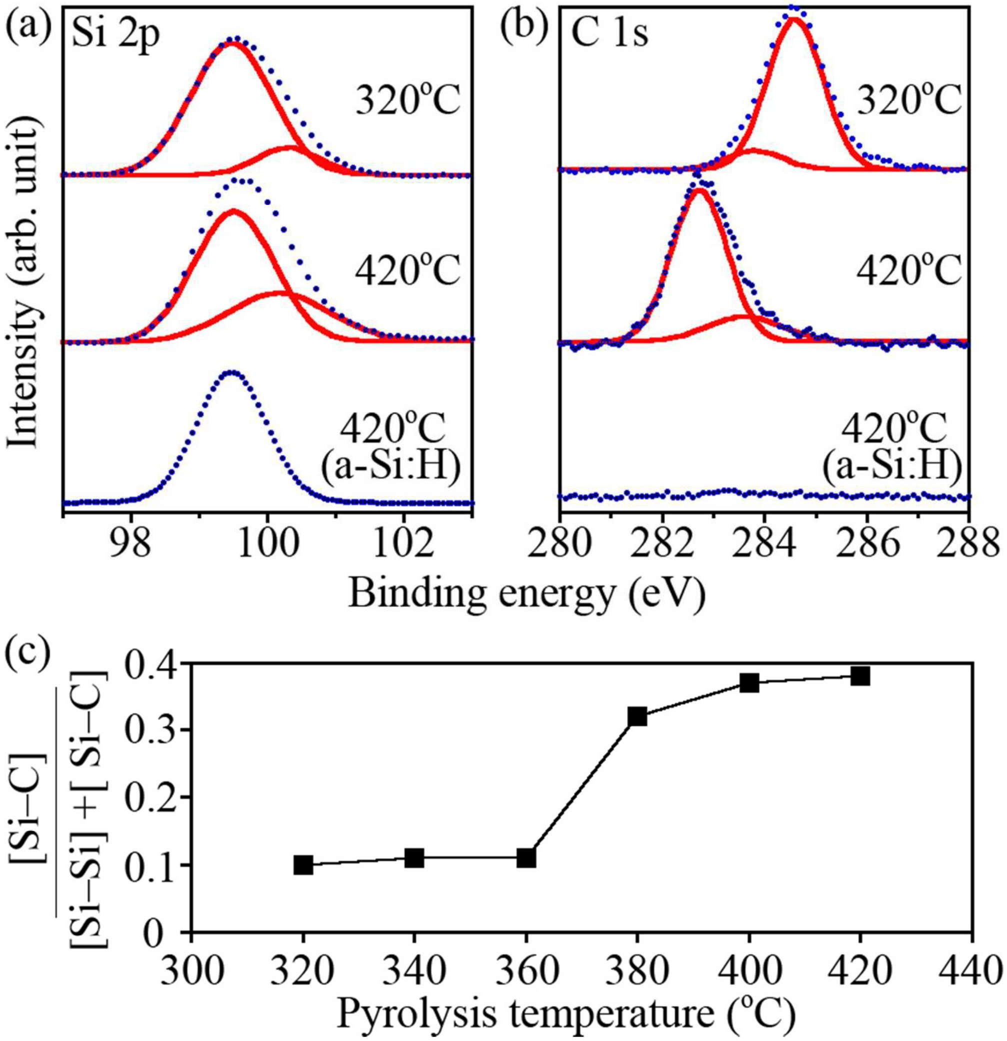

73x76mm (300 x 300 DPI)

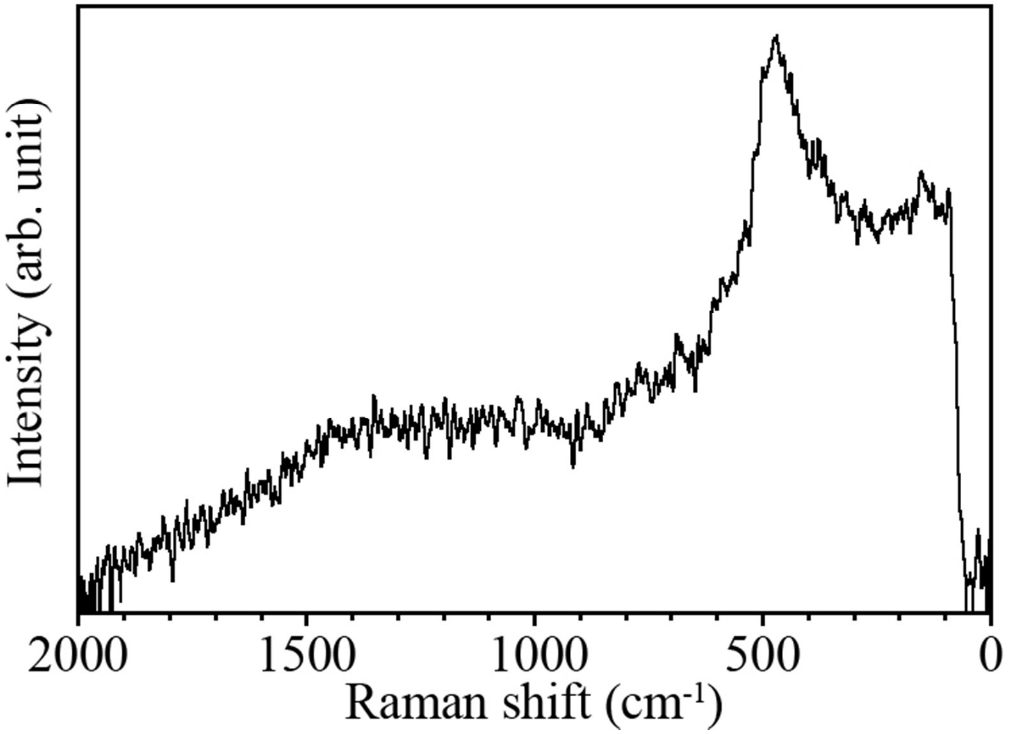

62x45mm (300 x 300 DPI)

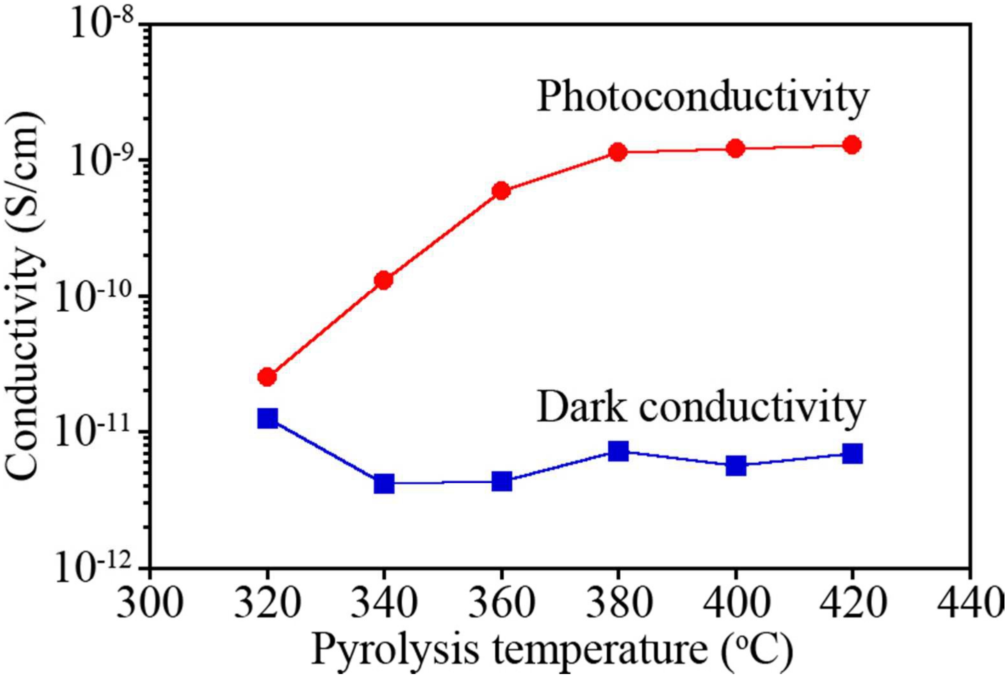

69x46mm (300 x 300 DPI)

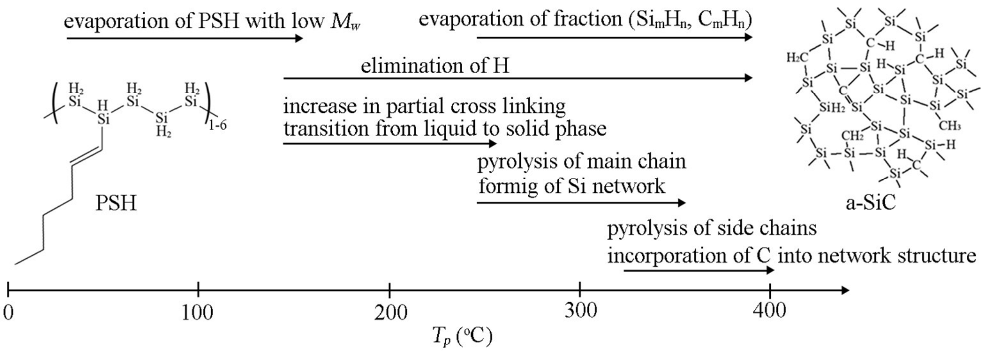

143x49mm (300 x 300 DPI)

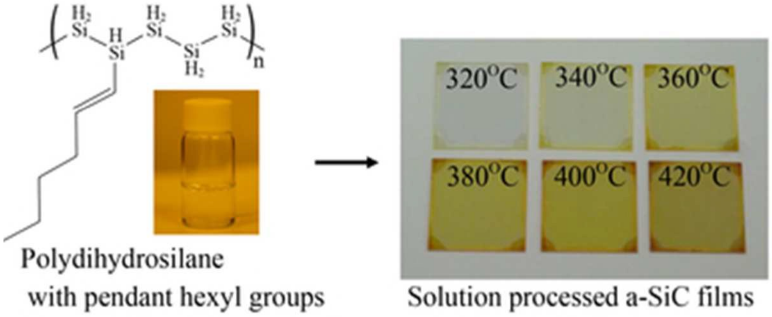

32x13mm (300 x 300 DPI)

Solution-processed a-SiC was realized using polymeric precursor. Polymer-to-ceramic conversion was investigated in this report.